PAPER • OPEN ACCESS

Two-bunch operation with ns temporal separation at the FERMI FEL facility

To cite this article: Giuseppe Penco *et al* 2018 *New J. Phys.* **20** 053047

New Journal of Physics
The open access journal at the forefront of physics

Deutsche Physikalische Gesellschaft DPG
IOP Institute of Physics

Published in partnership with: Deutsche Physikalische Gesellschaft and the Institute of Physics

OPEN ACCESS

RECEIVED
17 December 2017

REVISED
27 March 2018

ACCEPTED FOR PUBLICATION
26 April 2018

PUBLISHED
18 May 2018

PAPER

Two-bunch operation with ns temporal separation at the FERMI FEL facility

Giuseppe Penco[1], Enrico Allaria[1], Silvano Bassanese[1], Paolo Cinquegrana[1], Stefano Cleva[1], Miltcho B Danailov[1], Alexander Demidovich[1], Mario Ferianis[1], Giulio Gaio[1], Luca Giannessi[1,2], Claudio Masciovecchio[1], Mauro Predonzani[1], Fabio Rossi[1], Eleonore Roussel[1,3], Simone Spampinati[1] and Mauro Trovò[1]

[1] Elettra-Sincrotrone Trieste S.C.p.A., S.S. 14-km 163.5 in AREA Science Park 34149 Basovizza, Trieste, Italy
[2] ENEA C.R. Frascati, Via E. Fermi 45, I-00044 Frascati (Roma), Italy
[3] Present address: Laboratoire PhLAM, UMR CNRS 8523, Université Lille 1, Sciences et Technologies, 59655 Villeneuve d'Ascq, France.

E-mail: giuseppe.penco@elettra.eu

Keywords: free-electron laser, long-range wakefields, multi-bunch operation, pump–probe scheme

Abstract

In the last decade, a continuous effort has been dedicated to extending the capabilities of existing free-electron lasers (FELs) operating in the x-ray and vacuum ultraviolet regimes. In this framework, the generation of two-color (or multi-color) temporally separated FEL pulses, has paved the way to new x-ray pump and probe experiments and several two-color two-pulse schemes have been implemented at the main facilities, but with a generally limited time-separation between the pulses, from 0 to few hundreds of fs. This limitation may be overcome by generating light with two independent electron bunches, temporally separated by integral multiples of the radio-frequency period. This solution was investigated at FERMI, measurements and characterization of this two-bunch mode of operation are presented, including trajectory control, impact of longitudinal and transverse wakefields, manipulation of the longitudinal phase space and finally a demonstration of suitability of the scheme to provide extreme ultraviolet light by using both bunches.

1. Introduction

One of the challenges that scientists are facing in diverse research fields, consists in accessing the short time (femtosecond) and length-scales (nanometer) that characterizes the typical lifetime of transient states involved in many physical, chemical and bio-chemical processes [1]. Dynamical phenomena in physics, chemistry and biology, originate from similar mechanisms that involve motions of electrons, atoms, molecules and nanostructures. The recent advent of free-electron lasers (FEL) has boosted the development of techniques that could combine the short wavelength and time duration of the FEL photon pulses, in order to enter the femtosecond/nanometer dynamic region [2], with nonlinear XUV optics and photo correlation spectroscopy techniques. Two or more pulses are required to pump a given transient state in the sample and to monitor its temporal evolution. In the case of nonlinear experiments one of the quests is to have these two or more independent pulses to activate processes as sum frequency generation or four wave mixing [3, 4]. Photon correlation spectroscopy needs two identical pulses but with a time-delay that spans from hundreds of femtoseconds to hundreds of nanoseconds [5].

These demands are stimulating the development of innovative schemes for the generation of multiple pulses of multiple colors in XUV FELs. An FEL source producing a train of multiple pulses is not a novelty in FELs. Multiple pulses are naturally generated in oscillator FELs where the round trip time sets the lower repetition rate for the train of pulses, and multiple colors were also obtained in oscillators in pioneering experiments at CLIO [6] and Super-ACO [7]. In high gain single pass FELs several schemes have been implemented at LCLS [8–10], SACLA [11] and FERMI [12–15] with the goal of producing FEL light by two portions of the same electron bunch (at the same or different wavelengths), with a time-separation limited to few hundreds of fs. When two

sections of the radiator undulators are tuned at two distinct values of magnetic field in order to make the same electron bunch to lase twice, both FEL pulses have a limited intensity, that is lower than the saturation level. This limitation can be overcome by generating two independent electron bunches in the same rf bucket at the injector, with an initial time-separation of few ps. The two bunches are then accelerated in the linac and temporally compressed to tens of fs with the possibility to tune their temporal separation in the order of few tens of fs. This configuration was explored in Frascati at SPARC [16] and then implemented at LCLS in pump–probe experiments [17]. High gain FELs require however high-brightness electron beams which imply sub-micron transverse emittances and peak current of the order of kA, and the generation of two or more pulses has to deal with the strong wakefields and space charge effects coupling the bunches. The tuning of the linac setting is therefore by far more complicate than in the standard single bunch configuration. Emittance compensation and mitigation of space charge effects in the photoinjector is the result of a compromise between the injection phases of the two bunches and short-range wakefields induced by the drive bunch and acting on the trailing one affects the longitudinal compression and the bunches temporal separation.

All those schemes are limited by a maximum temporal separation of few hundreds fs and are definitely not suitable for pump and probe experiments requiring a time-delay of tens and hundreds of ps or in the ns range. A photon delay-line can in principle extend this range, but at the cost of a significant pulse energy loss and of reduced flexibility, e.g. limiting the operation to a set of predetermined wavelengths [18, 19].

The interest in producing ns time separated bunches has been growing since preliminary experiments performed at LCLS [20]. LCLS scientists have indeed investigated the SASE operation with multi-bunch separated from few ns to hundreds of ns, providing light for pump and probe experiments [21]. This option is also considered in the future operation of the SwissFEL [22], in order to enable parallel operation of the two FEL beam lines [23] and can be attracting for a FERMI future upgrade [24], allowing to operate simultaneously FEL-1 [25] and FEL-2 [26].

A further option, of particular interest at FERMI and FLASH [27], consists in exploiting the double-bunch mode in a configuration where one bunch is used by the FEL and the second one is used for THz emission, at FERMI hosted in a specifically dedicated beamline TeraFERMI [28]. The second bunch adds the possibility to control the relative delay in the tens of ns range and the order of arrival of the two pulses, and would be of primary importance in enabling pump–probe schemes which combine the THz and the XUV FEL pulses.

This multiple bunch operation may seem a simple and natural solution for a RF driven accelerator where in principle all the RF buckets can be filled by a bunch of charge. The generation of multiple electron bunches is however affected by collective effects such as wakefields or beam loading, that have to be analyzed and compensated to preserve the correct properties for lasing of both bunches. Those effects are particularly severe in case of high-impedance accelerating sections as occurs at FERMI or in the next generation linac facilities based on X-band technology.

For schemes aiming at an increase of the machine repetition rate by feeding different FEL lines with the multiple bunches as studied at LCLS and planned at SwissFEL, a time-separation of tens of ns between bunches is a viable option, allowing to correct the beam loading in the linac section by acting on the low level rf system [29] and to split the bunches by using very fast resonant magnetic kickers [30].

Conversely, in pump and probe configurations with few ns temporal delay, the above solutions are not feasible and it is necessary to operate the accelerator with two bunches with eventually slightly different energies. In a seeded and self-seeded FEL, there is an additional lasing condition on the k-vector of the emitted radiation, which is determined by the seed laser wavelength (in the former) and by the dispersive momentum selection of the monochromator (in the latter), and these detunings have to be accounted for. We have explored this configuration at FERMI, where the two independent electron bunches were separated by a multiple integer of the linac main radio-frequency (rf) period (≈333.6 ps), from 0.667 to 2.335 ns.

After a brief overview of FERMI, the next sections present the generation of two bunches at the photoninjector and the measurements and characterization of this mode of operation, including trajectory control, impact of longitudinal and transverse wakefields and the possibility to manipulate the electron longitudinal phase space by acting on the drive bunch charge or fine tuning the time-delay by few ps. The last section is finally devoted to describe the FEL lasing on the FEL-1 line [25] in the two-bunch mode by placing the seed laser on the drive or on the trailing bunch, showing a performance of the FEL output in terms of spectral bandwidth, intensity and stability very close to the ones in nominal operation.

2. FERMI

The experiments were carried out at FERMI [31], a FEL facility covering the VUV to soft x-ray photon energy range with two FELs, FEL-1 and FEL-2, both based on the high gain harmonic generation seeded mode [32]. The scheme consists in preparing the electron beam phase space in a first undulator, where the interaction with an

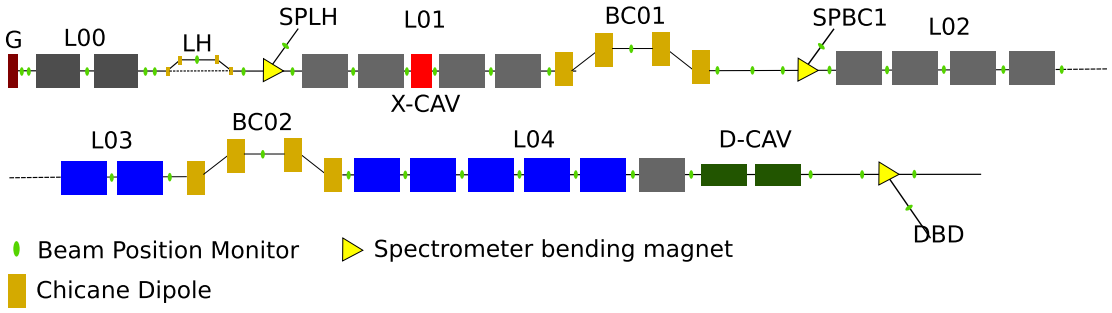

Figure 1. FERMI linac layout including the rf gun (G), the injector booster linac (L00), the laser heater (LH), the two-bunch compressors (BC1 and BC2), the rf deflecting cavities (D-CAV) and the linac L01, L02, L03 and L04, that are comprised of traveling wave (in gray) and backward traveling wave (in blue) accelerating sections. Green circles indicate the beam position monitors. There are three energy spectrometers beam lines, named SPLH, SPBC1 and DBD that is the diagnostic beam dump. The last one is exploited together with the vertical deflecting cavity to measure the electron longitudinal phase space.

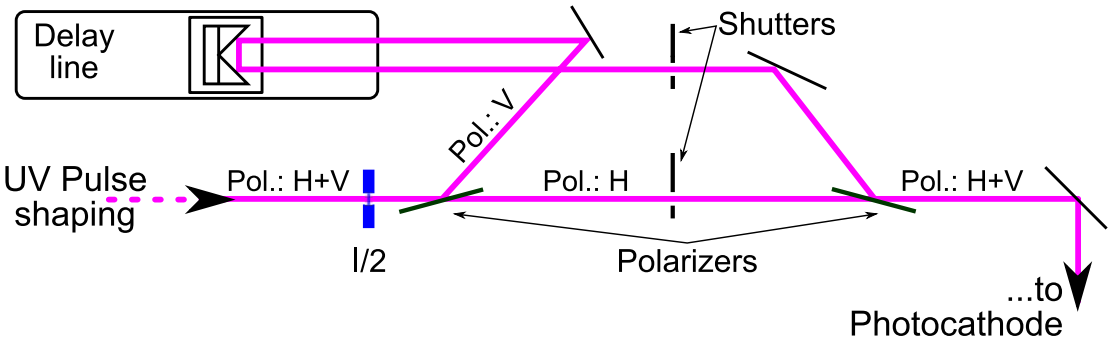

Figure 2. Photoinjector system modified for the two-bunch operation. The UV pulse is split by polarization and the intensity of each laser pulse is tuned by rotating the half-wave plate ($l/2$). Each pulse has an independent shutter.

external laser, the seed, induces a controlled and periodic modulation in the electron beam longitudinal energy distribution. A dispersive section converts the energy modulation into a density modulation, which is characterized by higher order harmonic components and retains the phase and amplitude properties of the seed. The density-modulated beam is then injected into a long FEL amplifier, similar to the one adopted in SASE FELs for the final amplification. FEL-1 covers the spectral range between 20 and 100 nm, in FEL-2 this process of harmonic conversion is repeated twice and the range of operation is between 20 and 4 nm. Both the FEL lines are driven by the same linac, as sketched in figure 1, starting from the photoinjector [33], the S-band accelerating sections, the two magnetic bunch compressors, the energy spectrometer beam lines and the deflecting cavities [34].

3. Photoinjector setup

The FERMI photoinjector laser (PIL) system is based on Ti:Sapphire as an active material and regenerative amplifier/multipass chirped-pulse amplifier design [35]. For the two-bunch experiment, the PIL system has been modified after the UV shaping. A schematic layout of the laser system is reported in figure 2. The UV pulse is split by polarization and the second pulse is driven through a delay-line introducing a temporal shift from 600 ps to 2.5 ns with respect to the first pulse. A rotating half-wave plate, placed before the splitting, is exploited to balance the energy between the two pulses. Finally each UV pulse has an independent shutter and the first or second bunch can be enabled or disabled independently. Similarly, the laser heater [36] pulse, that is directly generated from the PIL pulse, has been split in order to generate two pulses interacting with both electron bunches.

Our first goal in the two-bunch mode setup consisted in generating two bunches as much as possible mutually identical, since they had to share the same linac parameters setting. Therefore, the two laser pulses were tuned to achieve the same charge per bunch and with a separation exactly multiple of the main rf period, $\Delta T = N \times 333.6$ ps. We have then carried out a Schottky-scan, i.e. a measurement of the extracted charge versus the gun rf phase, sending in turn only one PIL pulse at the time (results plotted in figure 3). We have tuned

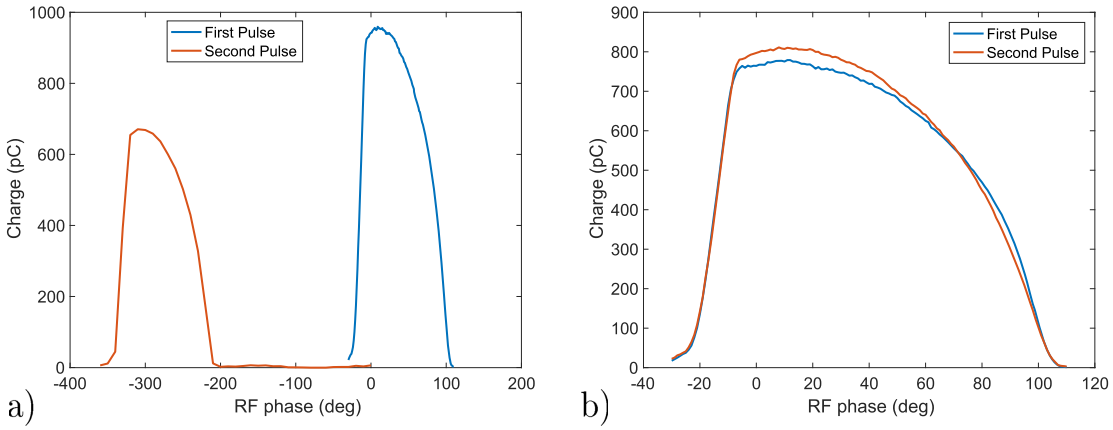

Figure 3. Schottky-scan performed sending in turn only one laser pulse on the cathode. The measurement was made before (a) and after (b) the fine tuning of the temporal delay ΔT and of the half-wave plate rotating angle.

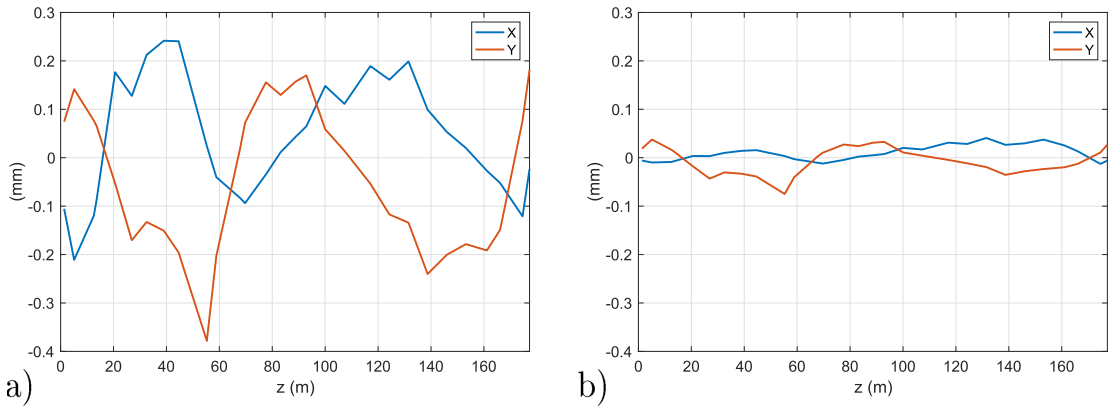

Figure 4. Second bunch (alone) trajectory along the linac before (a) and after (b) fine tuning the transverse position of the second PIL on the cathode. The reference trajectory (all reading at zero) corresponds to the first bunch trajectory obtained by sending only the first PIL pulse.

the temporal delay ΔT between the two pulses in order to have the same zero-charge extraction phase. Adjusting then the half-wave plate balancing the energy on the two arms to have the same laser intensity on the cathode allowed measuring two Schottky scans which were overlapping in time with the same shape (figure 3(b)). This has ensured that the two bunches were exactly the same when the gun rf phase is determined.

4. Trajectory control

The control of the beam trajectory is realized by a feedback system reading the beam position monitors distributed along the linac, highlighted by green circles in figure 1, and compensating the trajectory errors by applying orbit kicks resulting from a response matrix [37].

The initial condition of the beam trajectory is affected by the PIL pulses transverse alignment on the cathode. The two bunches orbit is then governed by the actual reading of the BPMs that see the two-bunch system as a whole, and by the effects of the long-range transverse and longitudinal wakefields (LRW) generated by the drive bunch on the trailing one.

4.1. PIL pulses alignment

It is mandatory to have a precise control of the transverse position of both PIL pulses on the cathode in order to make them coincident. A misalignment as small as $\approx$10 μm over a laser spot size of 0.65 mm (radius) leaded to $\approx$100 μm differences in the trajectories, as depicted in figure 4(a) for the case of $\Delta T = 0.667$ ns. The procedure used to introduce the second bunch was the following: after a rough alignment of the second PIL pulse on the cathode, we propagated only the drive bunch which was previously optimized by steering its trajectory to the reference (i.e. all BPMs reading at zero). Then we disabled the trajectory feedback and we propagated only the

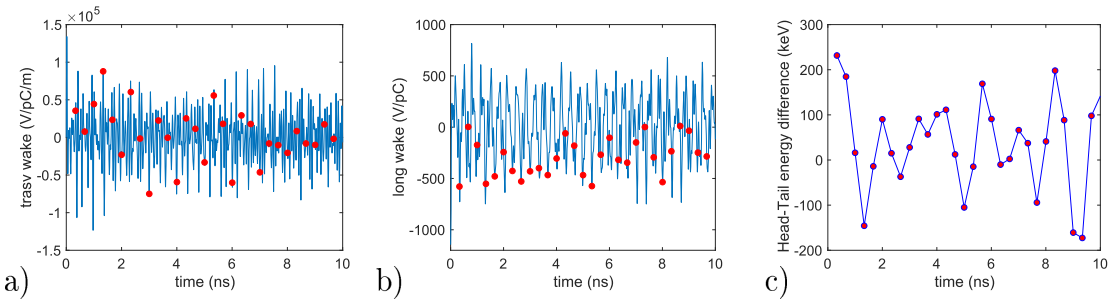

Figure 5. Simulated long-range transverse (a) and longitudinal (b) wake potential in one BTW section. Red circles correspond to the wake potential sampled by bunches in subsequent rf buckets. (c) Second bunch head-tail energy difference due to the long-range longitudinal wakefields induced in the seven BTW sections in subsequent rf buckets.

second bunch, which usually undergoes through a different trajectory (see figure 4(a)). At this point we moved the transverse position of the second PIL pulse on the cathode, steering with this handle the second bunch trajectory to the reference and minimizing the BPMs reading (see figure 4(b)).

Once this condition was set, operating with only the first bunch was equivalent to operating with the second bunch only: the measured optics and emittance along the linac of both bunches transported individually were very similar. However when both bunches were propagated, some issues concerning the BPMs response and the long-range wakefields (LRWs) effects, had to be addressed.

4.2. Beam position monitor

The bunch transverse position along the FERMI linac is detected by stripline BPMs, optimized to improve the response of the system for ps or sub-ps long electron bunches. The electronic signal generated by the bunch takes 1 ns to reach the short-circuit on a BPM edge and be reflected back. As a consequence a second bunch with a $\Delta T = 1$ ns perfectly cancels the electronic signal of the first one. We have indeed experienced a complete absence of signal on the BPMs for a $\Delta T = 1$ ns. The BPM signal excites a sixth-order band-pass filter at 500 MHz, (bandwidth $= 10$ MHz) with a resulting output oscillating pulse extending for hundreds of ns. Thus, an almost complete cancellation of the response signal occurs every 2 ns, defining a sequence of forbidden delays, $\Delta T = 1, 3, 5$ ns etc..., where the BPM reading is not reliable. In practice to be able to read the trajectory of the two-bunch system, we had to avoid the above time-delay series.

4.3. Long-range wakefields

The FERMI linac is comprised of two kinds of rf accelerating sections: SLAC-type traveling wave sections in the first part and backward traveling wave (BTW) sections in the second part [38]. When the beam passes through the latter, strong geometrical wakefields are excited due to their small iris [39] and during the trajectory optimization it is mandatory to minimize their effects. However, the transverse wakefields induced by the drive bunch and acting on the bunch itself (short-range) differ from those one acting on the trailing bunch (long-range). Thus, minimizing the former by steering the trajectory when only the drive bunch is propagated alone does not imply that the trajectory is the optimal one for the second bunch. In addition, the longitudinal LRW excited by the first bunch change the energy of the trailing bunch. This effect could in principle be compensated by shaping the rf pulse of the linac sections and/or acting on the low level rf system but it is feasible only for time-delay of several tens of ns. Nevertheless, provided that the energy difference is within the acceptance of the accelerator, two bunches with slightly different energies can be exploited in two-color FEL schemes [29]. In the following section we show that a small variation of the time-delay at the gun, of the order of few ps, can counteract the difference in energy between bunches without affecting the electron beam quality.

Figure 5 shows the longitudinal and transverse LRW potential calculated for the BTW sections by using ECHO code and MAFIA solver [39], and the temporal delays that are integer multiples of the main rf period are highlighted with red circles. According to the temporal delay the transverse LRW could be positive or negative, while the longitudinal LRW provide always a negative contribution, that means the trailer bunch has a lower energy than the drive bunch when ΔT is a multiple integer of the rf period.

After ensuring that the two bunches were equivalent in terms of charge, trajectory and timing relative to the rf phases, the two-bunch mode was enabled. We could not activate the transverse orbit feedback because it acted correcting the trajectory of the center of mass, kicking the first bunch off-axis, on the side enhancing the transverse wake generated on the second bunch. This resulted in an instability steering off-axis each bunch symmetrically and enhancing the transverse wake of the front bunch on the second. In the future, a technical solution may consist in dedicating a small fraction of shots to operate the drive bunch only with the trajectory

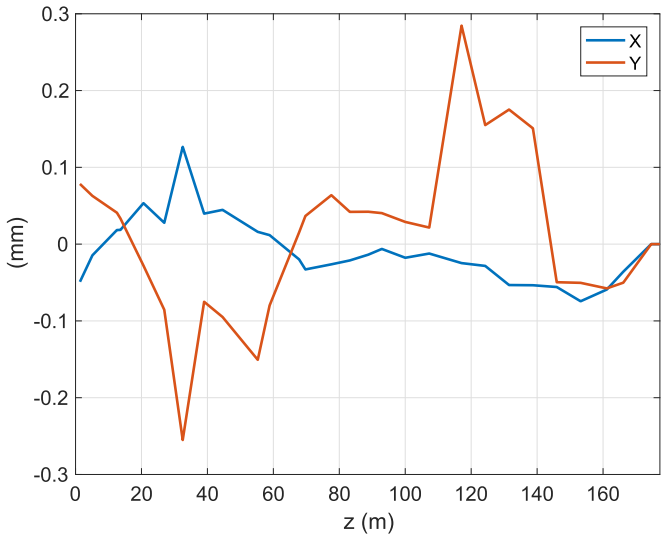

Figure 6. BPMs trajectory reading in two-bunch mode, when $\Delta T = 1.668$ ns.

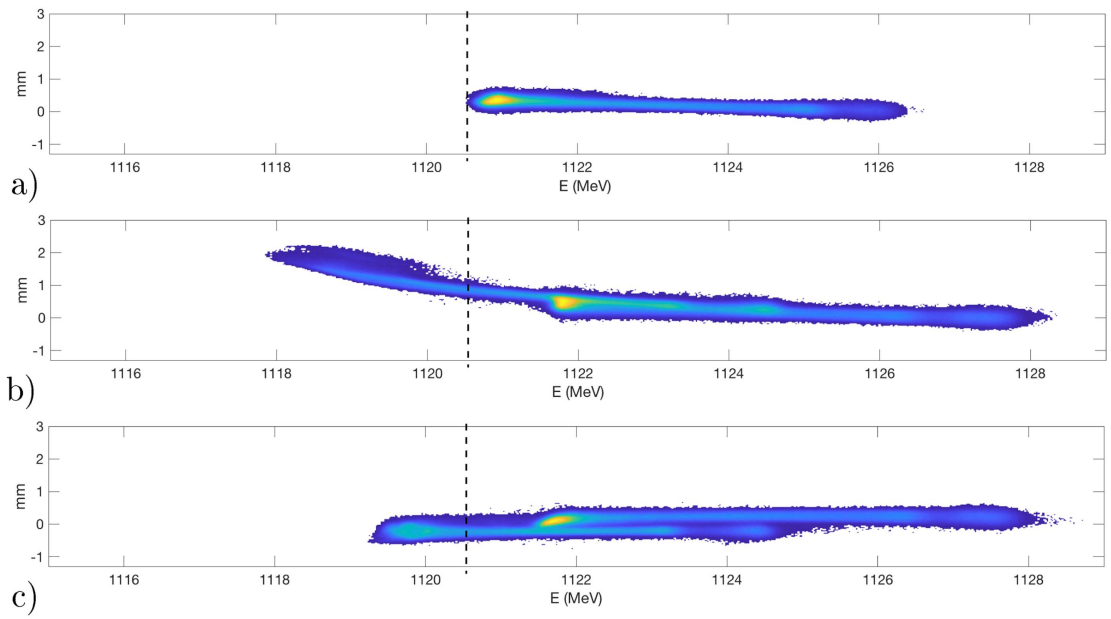

Figure 7. Energy distribution relative of a single bunch (a), and of the two bunches (b), (c) measured during the trajectory steering optimization. A vertical dotted line indicates the minimum energy of the drive bunch when it is propagated alone: in two-bunch mode the beam loading of the rf linac sections changes its energy. The temporal separation of the two bunches is 0.667 ns.

feedback enabled. Figure 6 reports the two-bunch system position along the linac as read by the BPMs for a temporal delay $\Delta T = 1.668$ ns, when the feedback were disabled: the trailer bunch was kicked off-axis by the transverse LRW induced by the drive bunch. We used the diagnostic screens placed along the linac to check the transverse position of both bunches, steering the first one and finding the best compromise for the trajectory of the second.

Sending the beam in the diagnostic beam dump (DBD) at the end of the linac allowed the simultaneous measurements of the vertical displacement of the two bunches and of their energy distributions. Figure 7 shows the energy distribution of the single bunch and of the two bunches during the steering optimization of the bunch drive trajectory, for a $\Delta T = 0.667$ ns. It is worth noting that the energy of the drive bunch changes when also the trailing bunch is co-propagated. This is an effect of the beam loading of the rf linac sections that is hard to be compensated in few rf cycles and strongly depends upon the temporal separation ΔT.

Figure 8 shows the energy distribution of both bunches measured in DBD versus ΔT. In addition to the short-range wakefields, the trailer bunch is affected by the long-range wakefields induced by the driver bunch

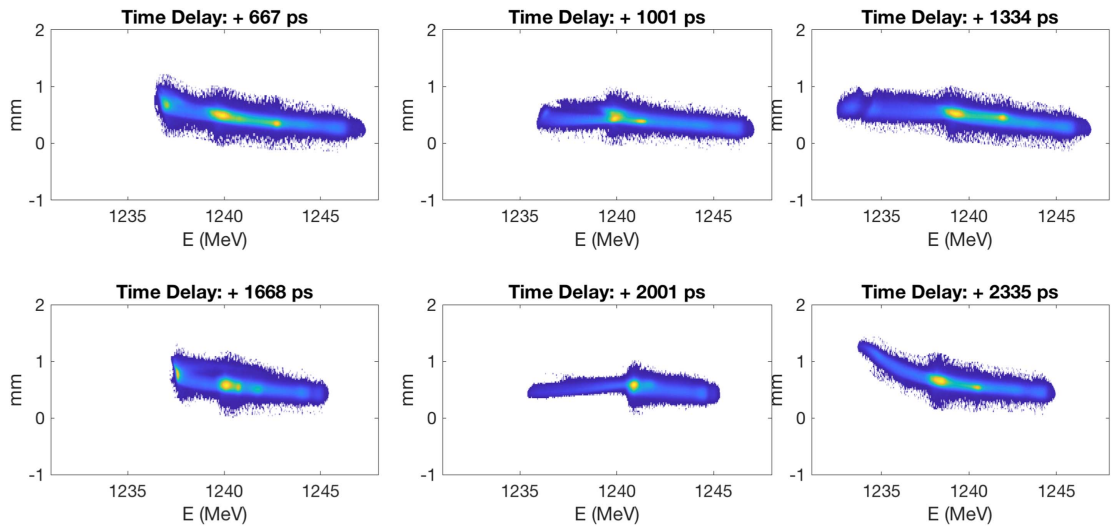

Figure 8. Energy distribution of the two bunches measured in DBD as a function of the temporal delay ΔT. The drive bunch is on the right and the trailing one is on the left.

that not only changes its energy centroid (see figure 5(b)) but even the energy distribution (see figure 5(c)). Despite being out of the scope of this paper, these measurements provide a method to estimate the long-range longitudinal wake potential from electron beam longitudinal phase space measurements.

The energy difference of few MeV over 1.2 GeV still allowed transporting the two bunches from the linac to the undulator and finally to the beam dump. The two bunches with different energy have different resonant wavelengths in the FEL, according to the condition:

$$\lambda_R = \frac{\lambda_u}{2\gamma^2}(1 + \alpha K^2), \tag{1}$$

where $K = eB_u\lambda_u/(2\pi m_e c)$ is the normalized undulator strength, λ_u and B_u are, respectively, the undulator period and peak magnetic field, α is 1 for helical undulator and 1/2 for planar undulator, and $\gamma m_e c^2$ is the electron energy.

5. Manipulation of the electron longitudinal phase space

The electron longitudinal phase space is routinely measured at the end of the linac, by combining the use of the rf deflector with the dispersion in the DBD [34]. The deflector stretches the beam vertically, imposing a correlation between the displacement of each electron and its temporal position, while the spectrometer disperses the particles horizontally according to their energy [40]. We used this tool to diagnose the individual characteristics of each bunch in the single and two-bunch configuration and to individually control the properties of the two bunches, e.g. to have one bunch with a peak current higher than the other one, for example to increase the power of the FEL light or the power of the THz radiation emitted by one of the bunches.

This may be achieved e.g. by tuning the temporal separation between the two PIL pulses. If the time-delay is slightly changed by few ps around an integer number of rf period, the trailing bunch samples a slightly different rf phase in the linac before the bunch compressor that together with the energy variation induced by the longitudinal wakefields changes the compression factor. Figure 9 shows the longitudinal phase space measured in DBD for two bunches temporally separated by two rf cycles (i.e. 0.667 ns) ± 1 ps, ± 3 ps, ± 5 ps. In figure 9 the current distributions of the two bunches are also reported in some of the aforementioned cases, highlighting the changes in the temporal profile of the trailer bunch. The drive bunch current distribution has slightly changed by one configuration to another probably due to fluctuations of the beam trajectory and machine parameters during the scan of the temporal delay (all feedback disabled).

Another important handle to control the properties of the two bunches are the bunch charges. An increase (decrease) of the drive bunch charge induces larger (smaller) longitudinal wakefields on the trailer bunch and has also an effect on the drive bunch itself, that has to propagate through the same linac but with a different charge. Figure 10 shows the longitudinal phase space of the two-bunch system for different charge of the drive bunch, keeping the trailer bunch at 700 pC and $\Delta T = 0.667$ ns. The trajectory and the machine setting had been optimized for a single bunch of 700 pC and the relative longitudinal phase space obtained in this condition is plotted in figure 10 (on the top-left).

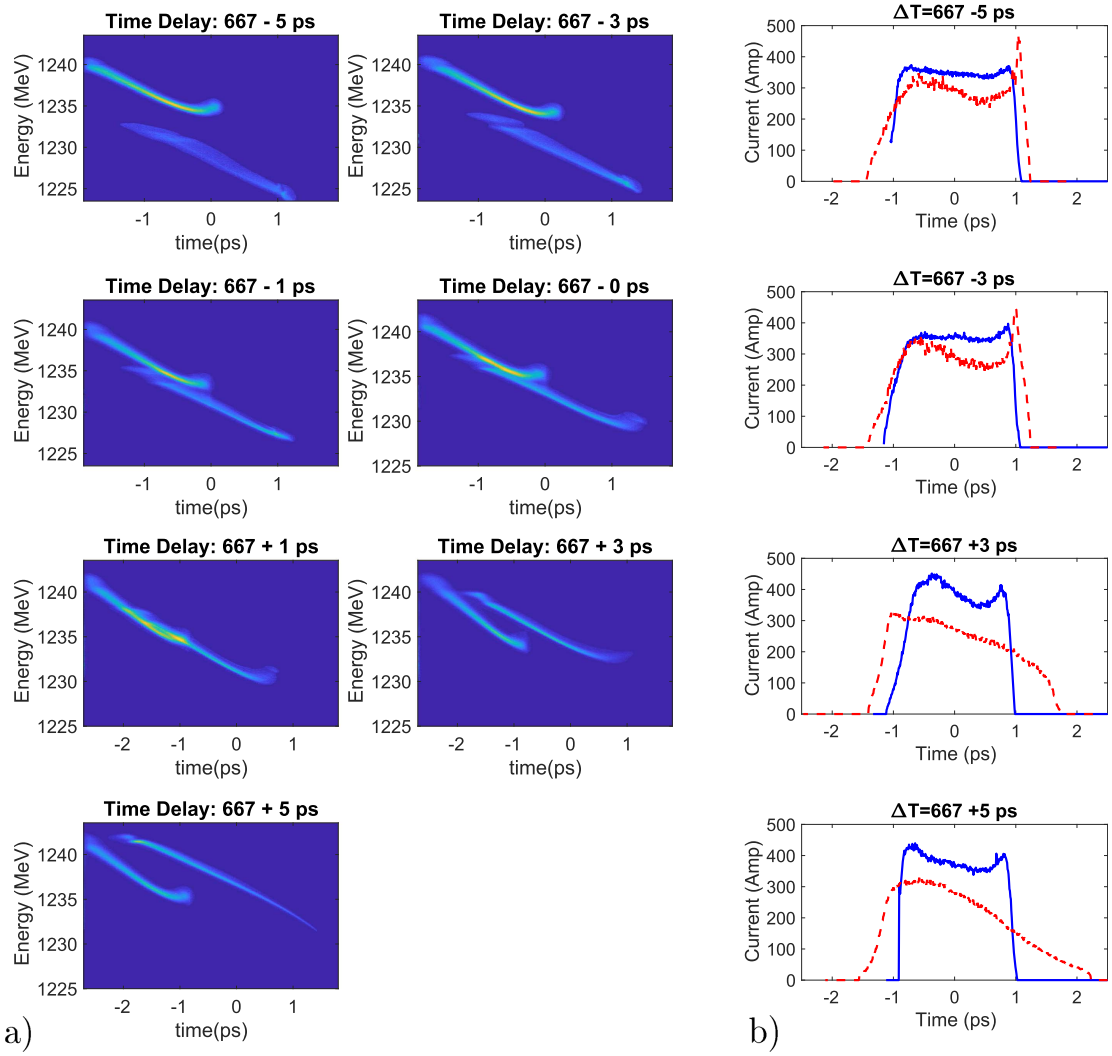

Figure 9. (a) Longitudinal phase space of the two bunches measured in DBD as a function of a small variation of the time-delay around 667 ps (from −5 to +5 ps). (b) Current profiles of the drive (in blue) and trailer (in red) bunch in four cases. Head of the bunch on the left.

Since the spatial delay between the bunches is much smaller than the linac sections length (∼3 m), both bunches induce a beam loading that is not compensated by the low level rf system. The final effect is a slightly increment of the accelerating gradient.

In the lack of transverse feedbacks, when the drive bunch has a different charge, it induces also a change in the short-range longitudinal wakefields: this leads to a slightly shifted trajectory in the magnetic bunch compressor, with a resulting different compression factor. Table 1 reports the energy and the horizontal position of the drive bunch in each case.

In all cases plotted in figure 10 the drive bunch is slightly shorter than the trailer one and this might be due to a non perfect adjustment of the two PIL pulses delay: the first bunch is generated with a small time-advance with respect to the second bunch, so that it samples a more compressing rf phase in the linac section before the BC1 chicane.

After the bunch compressor the higher the drive bunch charge the stronger the self-induced longitudinal wakefields, with a consequent increase of the linear and quadratic energy chirp in the time-energy distribution.

The changes in the longitudinal phase space of the trailer bunch is less evident and we have to isolate it from each plot of figure 10 and taking the mean energy of each temporal slice. The resulted energy–time curvature is reported in figure 11. An increment of the drive bunch charge increases the amplitude of the longitudinal LRW but this effect sums up with the aforementioned change of trajectory in the magnetic chicane. The latter changes the time of arrival of the drive bunch and consequently the time-delay between the two bunches. For this reason the linear energy chirp induced in the trailer bunch longitudinal phase space is not monotonic with the charge of the drive bunch.

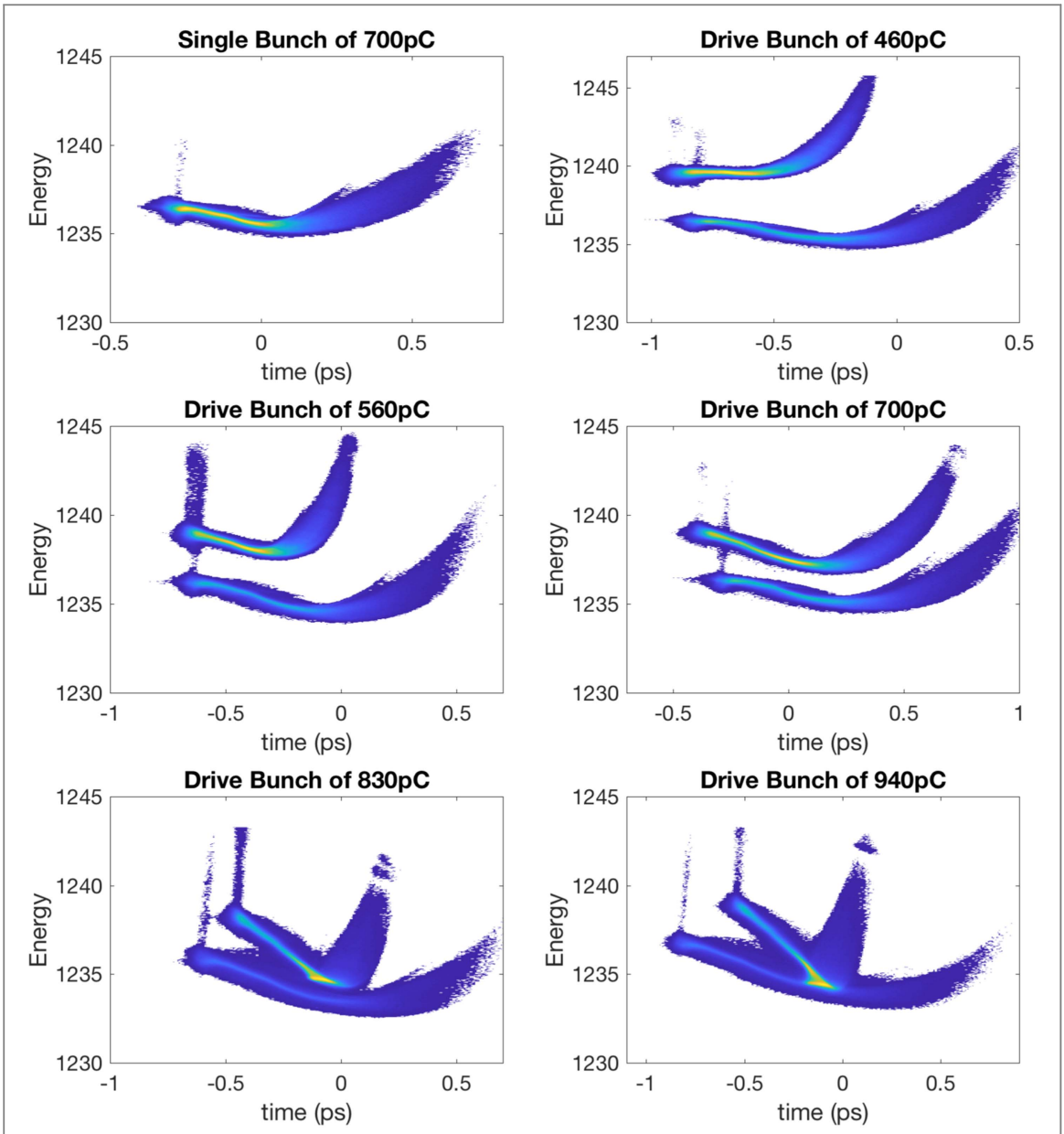

Figure 10. Longitudinal phase space of a 700 pC single bunch (on the top-left) and of two-bunch system (others graphs) when the drive bunch charge has been changed from 460 to 940 pC. The trailer bunch has always a smaller energy. Head of the bunch on the left. Temporal separation of 0.667 ns.

Table 1. Drive bunch energy and horizontal trajectory off-set in the BC1 chicane as a function of its charge.

Drive bunch charge (pC)	Energy (MeV)	Δx (mm)
460	279.8	0.75
560	279.9	0.66
700	280.6	0
830	280.6	−0.03
940	280.9	−0.38

In conclusion, the bunches charges and injection phases are tuning knobs which can be used to shape to some extent the two bunches phase spaces, partially compensating the energy differences, energy chirp and relative distances.

Figure 12 shows a series of energy–time curvature measured in subsequent shots in case of two bunches with 700 pC each and a temporal separation of 0.667 ns: the high shot-to-shot stability of the longitudinal phase space

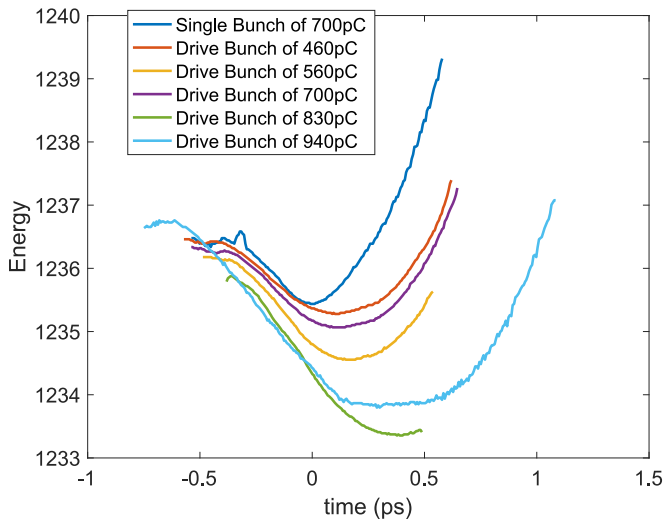

Figure 11. Trailer bunch energy–time dependence as a function of the drive bunch charge.

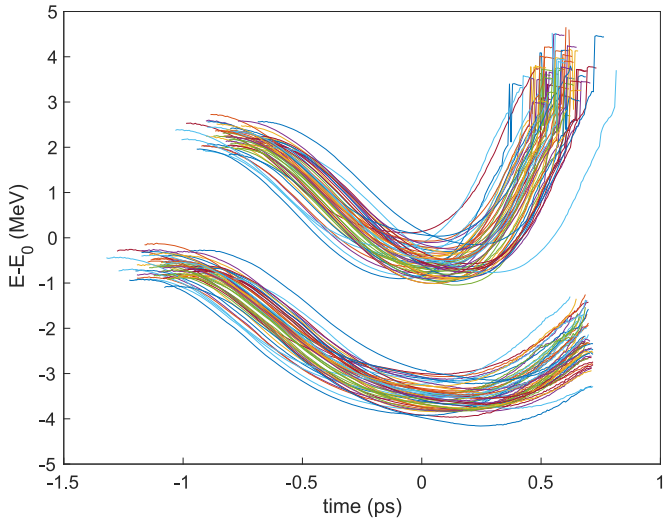

Figure 12. Shot-to-shot energy–time curvature of both bunches, with a temporal separation of 0.667 ns and a charge per bunch of 700 pC.

is very similar to the nominal single bunch case, with a measured mean energy jitter (rms) of about 0.02% for both bunches.

6. Free-electron laser with the trailer bunch

As a final test we explored the FEL operation in the double-bunch configuration. The two bunches with a $\Delta T = 0.667$ ns were injected in the undulator of the FERMI FEL-1 line. We could propagate the two bunches with small charge losses, similarly to the ones in the routine single bunch mode. The laser system in the setup used during the experiments did not allow the injection of two simultaneous seeds separated by the required temporal interval. We have therefore tested the efficiency of producing extreme UV pulses by alternately seeding the drive bunch or the trailer bunch. Since the FEL process only affects the properties (i.e. energy spread) of a small fraction of the electrons in the lasing bunch and does not produce any effects on the other bunch, this experiment is fully equivalent to having two distinct seed lasers.

Figure 13 reports a sequence of single-shot FEL spectra at about 62 nm acquired in different cases.

First of all the seed laser has been temporally overlapped on the drive bunch, obtaining an FEL output very similar to the nominal condition, with a spectral bandwidth of 4.7×10^{-4} and an intensity stability (rms) of ~19% (see figure 13(a)). Then, the seed laser has been temporally moved on the trailer bunch and after a

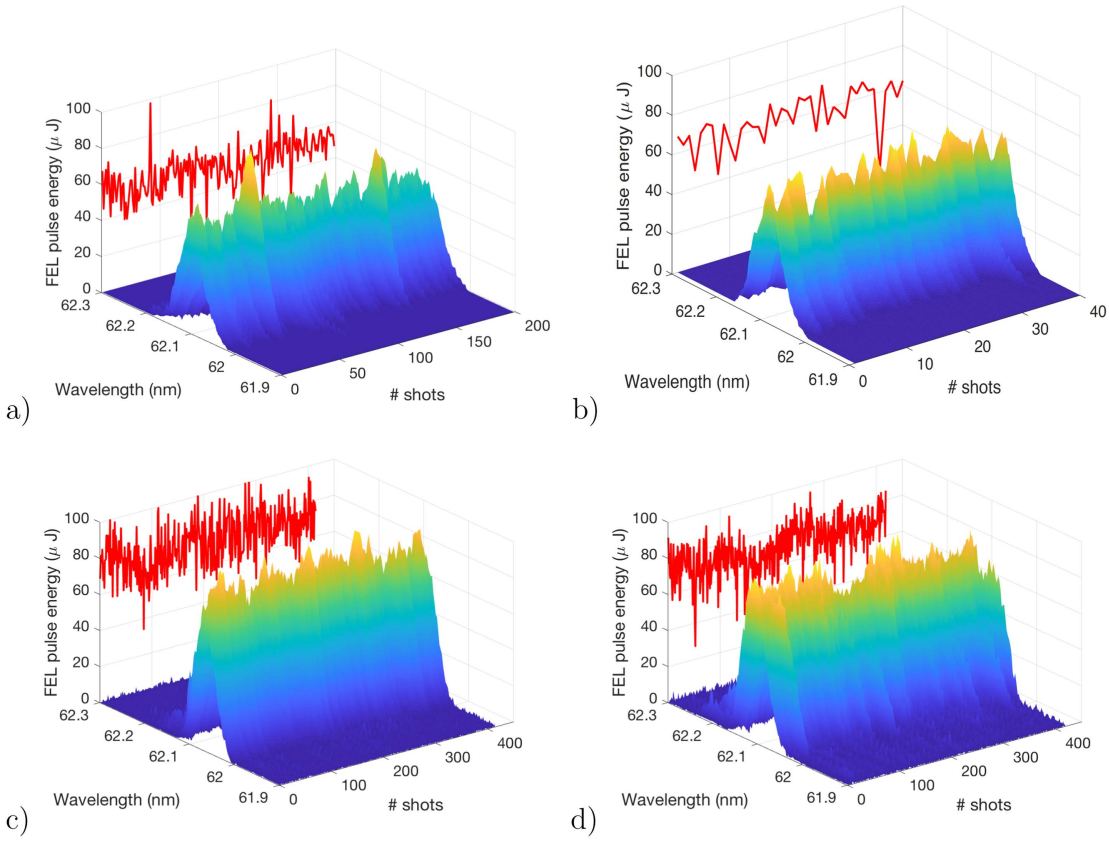

Figure 13. Shot-to-shot FEL spectra obtained by seeding the 700 pC drive bunch (a) or the 700 pC trailer bunch when the charge of the former is 700 (b), 550 (c) or 480 pC (d). FEL pulse energy is reported on the *z*-axis in red. The shot-to-shot FEL energy per pulse stability in the four cases are ~19% (a), ~16% (b), ~15% (c), (d). Temporal separation between bunches was set at 0.667 ns.

machine optimization needed to match the trailer bunch energy with the undulator magnetic field (less than 1%), we have obtained a very similar FEL output, with a spectral bandwidth of 5.0×10^{-4}, a mean pulse energy of 60 μJ over 40 shots and an intensity stability of ~16% rms (see figure 13(b)).

As described in the previous section, some machine configurations could benefit from having two bunches with different charges. Thus, it has been worthwhile to characterize the FEL performance also when the drive bunch has a different charge. We have therefore decreased the drive bunch charge down to 550 pC and to 480 pC, acquiring the FEL spectra produced by seeding the 700 pC trailer bunch (see figures 13(c), (d)). Even in these two configurations the FEL performance were close to the nominal one, with a spectral bandwidth of 3.8×10^{-4} (for the 550 pC case) and 4.2×10^{-4} (for the 480 pC case). The improvement of the mean pulse energy with respect to the case depicted in figure 13(b) was mainly due to a better optimization of the machine parameters.

These experiments demonstrate the suitability of the scheme for generating not only two-color FEL pulses but even multi-color FEL pulses, by adopting one of the scheme mentioned in the introduction [12, 15] or a combination of them. In fact it is possible to use two seed lasers with slightly different wavelengths in order to match the energy of each bunch, keeping the same undulators setting, or splitting the radiator in distinct portions tuned at different harmonic of each seed for a larger flexibility.

7. Conclusion

At FERMI we have experimentally demonstrated the possibility to generate two electron bunches, with a time-delay from 0.667 to 2.335 ns, that have been accelerated and compressed to few hundreds of fs and sent through the FEL-1 undulator line up to the main beam dump. The long-range wakefields induced in the linac sections by the drive bunch and affecting the trajectory and energy of the trailing bunch have been studied. Fine tuning the drive bunch charge and/or the time-delay between the bunches has allowed to manipulate the longitudinal phase space of both bunches, opening the door to novel machine configurations.

We have lased on the FEL-1 line in the two-bunch mode by placing the seed laser on the drive or on the trailing bunch, obtaining an FEL output very close to the nominal condition in terms of spectral bandwidth,

intensity and energy stability. This experiment has proven that two-color two-pulse FEL with few ns temporal separation could be generated by using two independent seed lasers. As a forthcoming application not implying any modification to the seed laser system, we seek the possibility of using the second bunch for the FEL emission and the first one for producing synchronized THz light in the TeraFERMI line, which could be temporally superimposed to the UV pulse, paving the way for THz-pump FEL-probe experiments.

Acknowledgments

The authors are grateful to the FERMI control team, the radio-protection team, the commissioning and operation team for the valuable support during the machine setting and optimisation and to the PADReS team for taking care of the photon transport and spectrometer setup during the FEL measurements.

ORCID iDs

Giuseppe Penco https://orcid.org/0000-0002-4900-6513
Enrico Allaria https://orcid.org/0000-0001-9570-6361

References

[1] Zewail A W 2000 *Pure Appl. Chem.* **72** 2219–31
[2] Bencivenga F, Capotondi F, Principi E, Kiskinova M and Masciovecchio C 2015 *Adv. Phys.* **63** 327–404
[3] Glover T E *et al* 2012 *Nature* **488** 603–8
[4] Bencivenga F *et al* 2015 *Nature* **520** 205–8
[5] Grübel G, Stephenson G B, Gutt C, Sinn H and Tschentscher T 2007 *Nucl. Instrum. Methods Phys. Res.* A **262** 357–67
[6] Prazeres R, Glotin F, Insa C, Jaroszynski D A and Ortega J M 1998 *Nucl. Instrum. Methods Phys. Res.* A **407** 464–9
[7] Renault E, Nahon L, Nutarelli D, Garzella D, Merola F and Couprie M E 2000 *Proc. SPIE* **3925** 29–39
[8] Lutman A A *et al* 2013 *Phys Rev. Lett.* **110** 134801
[9] Marinelli A *et al* 2013 *Phys Rev. Lett.* **111** 134801
[10] Lutman A *et al* 2016 *Nat. Photonics* **10** 745
[11] Hara T *et al* 2013 *Nat. Commun.* **4** 2919
[12] Allaria E *et al* 2013 *Nat. Commun.* **4** 2476
[13] De Ninno G *et al* 2013 *Phys. Rev. Lett.* **110** 064801
[14] Mahieu B *et al* 2013 *Opt. Express* **21** 022728
[15] Ferrari E *et al* 2016 *Nat Commun.* **7** 10343
[16] Petralia A *et al* 2015 *Phys. Rev. Lett.* **115** 014801
[17] Marinelli A *et al* 2015 *Nat. Commun.* **6** 6369
[18] Joksch S, Graeff W, Hastings J B and Siddons D P 1992 *Rev. Sci. Instrum.* **63** 1114
[19] Roseker W *et al* 2011 *Synchrotron Radiat.* **18** 481
[20] Decker F-J *et al Proc. FEL2010 Conf.* WEPB33
[21] Seaberg M H *et al* 2017 *Phys. Rev. Lett.* **119** 067403
[22] Schietinger T *et al* 2016 *Phys. Rev. Accel. Beams* **19** 100702
[23] Pedrozzi M 2010 *SwissFEL Injector Conceptual Design Report,* PSI Report Nr. 10-05 Paul Scherrer Institut
[24] Svandrlik M *et al* 2017 *Proc. IPA2017 Conf.*WEPAB039
[25] Allaria E *et al* 2012 *Nat. Photonics* **6** 699
[26] Allaria E *et al* 2013 *Nat. Photonics* **7** 913
[27] Schreiber S and Klose K 2017 *Proc. FEL2017 Conf.* WEP002
[28] Perucchi A *et al* 2013 *Rev. Sci. Instrum.* **84** 022702
[29] Decker F-J *et al Proc. FEL2015 Conf.* WEP023
[30] Paraliev M, Gough C, Dordevic S and Braun H 2015 *Proc. FEL2015 Conf.*MOP039
[31] Allaria E *et al* 2015 *J. Synchrotron Radiat.* **22** 485–91
[32] Yu L H 1991 *Phys. Rev.* A **44** 5178
[33] Penco G *et al* 2013 *JINST* **8** P05015
[34] Craievich P *et al* 2015 *IEEE Trans. Nucl. Sci.* **62** 1–11
[35] Danailov M *et al* 2007 *Proc. FEL 2007 Conf.,* WEPPH014
[36] Spampinati S *et al* 2014 *Phys. Rev. ST Accel. Beams* **17** 120705
[37] Gaio G and Lonza M 2013 *Proc. ICALEPCS2013 Conf.*THPPC129
[38] Di Mitri S *et al* 2009 *Nucl. Instrum. Methods Phys. Res.* A **608** 19
[39] Craievich P, Weiland T and Zagorodnov I 2006 *Nucl. Instrum. Methods Phys. Res.* A **558** 58–61
[40] Penco G *et al* 2012 *Proc. FEL2012 Conf.*WEPD20